HHS Public Access

Author manuscript

Nature. Author manuscript; available in PMC 2014 August 11.

Published in final edited form as:

Nature. 2013 December 5; 504(7478): 143–147. doi:10.1038/nature12830.

Oncogenic *Nras* has bimodal effects on stem cells that sustainably increase competitiveness

Qing Li[1,5], **Natacha Bohin**[#1], **Tiffany Wen**[#1], **Victor Ng**[1], **Jeffrey Magee**[2], **Shann-Ching Chen**[3], **Kevin Shannon**[4], and **Sean J. Morrison**[2,5]

[1]Department of Medicine, University of Michigan, Ann Arbor, Michigan 48109, USA

[2]Howard Hughes Medical Institute, Department of Pediatrics, and Children's Research Institute, University of Texas Southwestern Medical Center, Dallas, Texas, 75390, USA

[3]Department of Pathology, St Jude Children's Research Hospital, Memphis, Tennessee, USA

[4]Department of Pediatrics, University of California San Francisco, San Francisco, California 94158, USA

[#] These authors contributed equally to this work.

Abstract

"Pre-leukemic" mutations are thought to promote clonal expansion of haematopoietic stem cells (HSCs) by increasing self-renewal and competitiveness[1]; however, mutations that increase HSC proliferation tend to reduce competitiveness and self-renewal potential, raising the question of how a mutant HSC can sustainably outcompete wild-type HSCs. Activating mutations in *NRAS* are prevalent in human myeloproliferative neoplasms and leukemia[2]. Here we show that a single allele of oncogenic $Nras^{G12D}$ increases HSC proliferation but also increases reconstituting and self-renewal potential upon serial transplantation in irradiated mice, all prior to leukemia initiation. $Nras^{G12D}$ also confers long-term self-renewal potential upon multipotent progenitors. To explore the mechanism by which $Nras^{G12D}$ promotes HSC proliferation and self-renewal we assessed cell cycle kinetics using H2B-GFP label retention and BrdU incorporation. $Nras^{G12D}$ had a bimodal effect on HSCs, increasing the rate at which some HSCs divide and reducing the rate at which others divide. This mirrored bimodal effects on reconstituting potential as rarely dividing $Nras^{G12D}$ HSCs outcompeted wild-type HSCs while frequently dividing $Nras^{G12D}$ HSCs did not. $Nras^{G12D}$ had these effects by promoting STAT5 signaling, inducing different transcriptional responses in different subsets of HSCs. One signal can therefore increase HSC proliferation, competitiveness, and self-renewal through bimodal effects on HSC gene expression, cycling, and reconstituting potential.

[5]Co-Corresponding Authors: Qing Li (lqing@umich.edu) and Sean Morrison (Sean.Morrison@UTSouthwestern.edu).

AUTHOR CONTRIBUTIONS Q.L performed most of the experiments. N.B., T.W. and V.N. performed some of the experiments with help from Q.L. J.M. performed the western analysis of *Pten* mutant cells. S.C performed statistical analysis of microarrays. Q.L., K.S., and S.J.M. conceived the project, designed experiments, interpreted results, and wrote the manuscript.

COMPETING INTERESTS The authors declare no competing financial interests.

To gain a durable competitive advantage, mutant HSCs must sustainably self-renew more frequently than wild-type HSCs. Yet increased HSC division is almost always associated with reduced self-renewal potential and HSC depletion[3–5]. Many oncogenic mutations increase HSC proliferation but deplete HSCs, preventing clonal expansion[6]. Some oncogenic mutations do increase HSC self-renewal, including over-expression of *Ezh2*[7] or *Csf3r* truncation[8], and deletion of *p18*^{INK4C} [9], *Tet2*[10], *Dnmt3a* [11] or *Lnk* [12,13]. However, it remains uncertain whether these mutations can account for pre-leukemic expansion.

Human leukemias commonly have mutations that increase Ras signaling, including *NRAS* or *KRAS2* point mutations[2]. Mouse models with conditional expression of oncogenic *Kras*^{G12D} develop a rapid onset, aggressive myeloproliferative neoplasm (MPN) [14,15]. Kras^{G12D} drives HSCs into cycle and reduces HSC frequency [14,15]. *Nras*^{G12D} knock-in mice, on the other hand, develop an indolent MPN with delayed onset and prolonged survival [16,17]. NF1 inactivation[18] or *Nras*^{G12D} expression[17,19] allow bone marrow cells to out-compete wild-type cells in transplantation assays but it remains unclear whether they promote sustained pre-leukemic expansion, or how that might occur.

To conditionally activate a single allele of *Nras*^{G12D} in HSCs we generated *Mx-1-Cre; Nras*$^{G12D/+}$ mice in which the oncogenic *G12D* mutation was knocked into the endogenous *Nras* locus along with a floxed stop cassette[20]. To induce *Nras*^{G12D} expression, mice were administered poly-inosine:poly-cytosine (pIpC) at 6-10 weeks after birth (Extended data Figure 1). At 2 weeks and 3 months after pIpC treatment, more than twice as many *Nras*$^{G12D/+}$ CD150^{+}CD48^{-}Lineage^{-}Sca-1^{+}c-kit^{+} (CD150^{+}CD48^{-}LSK) HSCs[21] incorporated a 24-hour pulse of bromo-deoxyuridine (BrdU) as compared to control HSCs ($p<0.01$; Figure 1a). Consistent with this, twice as many *Nras*$^{G12D/+}$ HSCs were in G1 phase of the cell cycle as compared to control HSCs (Extended data Figure 1b). This increase in HSC proliferation did not significantly affect the number of HSCs or multipotent progenitors (MPPs) two weeks after *Nras*^{G12D} activation (Figure 1c). However, *Mx-1-Cre; Nras*$^{G12D/+}$ mice had significantly more LSK cells in the bone marrow and spleen (Figure 1c). We also observed a two-fold increase in BrdU incorporation in HSCs as well as an expansion of LSK cells in *Vav1-Cre; Nras*$^{G12D/+}$ mice as compared to controls (Figure 1b; Extended data Figure 2a). Thus *Nras*^{G12D} increased HSC division and expanded the pool of primitive hematopoietic progenitors.

To test competitiveness we transplanted 5×10^5 whole bone marrow cells from *Mx-1-Cre; Nras*$^{G12D/+}$ or control donors into irradiated wild-type recipients along with 5×10^5 recipient bone marrow cells. The *Nras*$^{G12D/+}$ cells gave significantly higher levels of reconstitution than control cells in all lineages for at least 20 weeks after transplantation (Figure 1d). In recipients of control donor cells, 69±13% of HSCs, 47±12% of MPPs, and 44±12% of LSK cells were donor-derived (Figure 1e); however, in recipients of *Nras*$^{G12D/+}$ donor cells 93±8% of HSCs, 90±8% of MPPs, and 85±15% of LSK cells were donor-derived (Figure 1e). *Nras*$^{G12D/+}$ HSCs therefore outcompeted wild-type HSCs.

To further test whether *Nras*$^{G12D/+}$ HSCs could outcompete wild-type HSCs we transplanted 10 CD150^{+}CD48^{-}LSK donor HSCs from the bone marrow of *Mx-1-Cre; Nras*$^{G12D/+}$ or littermate control mice (2 weeks after finishing pIpC) into irradiated wild-

type recipients along with 3×10^5 recipient bone marrow cells. The *Nras*$^{G12D/+}$ HSCs gave significantly higher levels of reconstitution compared to control donor HSCs in all lineages for at least 20 weeks after transplantation (Figure 1f).

To assess self-renewal potential we serially transplanted 3×10^6 whole bone marrow cells from three or four recipients per treatment into 2–5 irradiated mice per recipient (depending on the number of bone marrow cells we recovered) during each round of transplantation. In secondary, tertiary, and quaternary recipient mice we continued to observe significantly higher levels of reconstitution from the *Nras*$^{G12D/+}$ donor cells than from control donor cells in all lineages (Figure 2a–c). In tertiary recipient mice the control cells gave only transient multilineage reconstitution as they appeared to exhaust their self-renewal potential. In contrast, the *Nras*$^{G12D/+}$ HSCs gave high levels of long-term multilineage reconstitution in all 9 tertiary recipients, suggesting increased self-renewal potential. In quaternary recipient mice *Nras*$^{G12D/+}$ donor cells continued to give long-term multilineage reconstitution in most recipients while control donor cells gave only low levels of transient lymphoid reconstitution (Figure 2c). *Nras*^{G12D} thus increased the self-renewal potential of HSCs in addition to increasing their rate of division (Figure 1a) and their ability to compete with wild-type HSCs (Figure 1d, f).

A fifth round of transplantation from four quaternary recipients of *Nras*$^{G12D/+}$ cells did not yield any multilineage reconstitution by donor cells in the recipient mice (Extended data Figure 3). *Nras*$^{G12D/+}$ HSCs, therefore, eventually exhausted their self-renewal potential despite self-renewing more than control cells. Serial transplantation of *Vav1-Cre; Nras*$^{G12D/+}$ whole bone marrow cells showed that *Nras*$^{G12D/+}$ significantly increased HSC competitiveness in this genetic background as well (Extended data Figure 2b and 2c).

To test whether *Nras*^{G12D} expression influenced the reconstituting potential of MPPs we transplanted 10 donor CD150$^-$CD48$^-$LSK cells[22] from the bone marrow of *Mx-1-Cre; Nras*$^{G12D/+}$ or littermate control mice (2 weeks after finishing pIpC) into irradiated recipients along with 3×10^5 recipient bone marrow cells. Only one of 14 recipients of control MPPs exhibited long-term multilineage reconstitution by donor cells (Extended data Figure 4a). In contrast, 8 of 17 recipients of *Nras*$^{G12D/+}$ MPPs were long-term multilineage reconstituted by donor cells. *Nras*$^{G12D/+}$ MPPs were thus significantly ($p<0.01$ across three independent experiments) more likely to give long-term multilineage reconstitution than control MPPs.

Nras^{G12D} did not detectably affect the reconstituting potential of 25 CD150$^+$CD48$^+$LSK cells or 100 CD150$^-$CD48$^+$LSK cells (which contain restricted myeloid progenitors[22]) upon transplantation into irradiated mice (Extended data Figure 4b and 4c). *Nras*$^{G12D/+}$ thus increases the self-renewal potentials of HSCs and MPPs but not necessarily other progenitors.

We did not detect any evidence of leukemia or MPN in any of the recipient mice from the first, second, third, or fourth rounds of serial transplantation in terms of blood cell counts (Extended data Figure 5) or histology (data not shown). Only two recipients of *Nras*$^{G12D/+}$

cells and two recipients of control cells died spontaneously in these experiments. The effects of *Nras*$^{G12D/+}$ on HSC function therefore occurred in the absence of leukemogenesis.

To assess the effect of *Nras*$^{G12D/+}$ on HSC cycling over time we mated the *Mx1-cre*; *Nras*$^{G12D/+}$ mice with *Col1A1-H2B-GFP; Rosa26-M2-rtTA* double transgenic mice [4]. These mice allowed us to label HSCs with H2B-GFP during a 6 week period of doxycycline administration and then to follow the division history of all cells in the HSC pool as they diluted H2B-GFP with each round of division during a subsequent 12–15 week chase without doxycycline.

Two weeks after pIpC treatment, *Mx1-cre; Nras*$^{G12D/+}$; *Col1A1-H2B-GFP; Rosa26-M2-rtTA* mice and *Nras*$^{G12D/+}$; *Col1A1-H2B-GFP; Rosa26-M2-rtTA* controls (lacking *Cre*) exhibited similar background levels of GFP fluorescence (Figure 3a). After treating the mice with doxycycline for 6 weeks, all HSCs were strongly GFP^{+} (Figure 3a). *Mx1-cre; Nras*$^{G12D/+}$ and control HSCs exhibited indistinguishable levels of H2B-GFP labeling immediately after doxycycline treatment (Figure 3a). After a 12-week chase without doxycycline, the *Nras*^{G12D} and control HSCs exhibited a wide range of GFP expression levels (Figure 3b). In contrast, most bone marrow cells from *Mx1-cre; Nras*$^{G12D/+}$ and control mice exhibited GFP levels similar to background (Extended data Figure 6a). To assess the frequencies of HSCs that were most infrequently cycling, most frequently cycling, and moderately cycling we determined the frequencies of H2B-GFP^{hi} HSCs (with GFP levels similar to freshly labeled cells, see Figure 3a), H2B-GFP^{-} HSCs (with little or no GFP expression above background, see Figure 3a), and H2B-GFP^{lo} HSCs (with intermediate levels of GFP), respectively. In eight independent experiments, *Nras*^{G12D} significantly ($p<0.05$ by two-way ANOVA) increased the frequencies of both the H2B-GFP^{-} frequently cycling HSCs and the H2B-GFP^{hi} infrequently cycling HSCs in every pair of mice we examined (n=8) (Figure 3b). There was a corresponding significant decrease in the frequency of H2B-GFP^{lo} HSCs in *Nras*^{G12D} mice.

The median level of GFP fluorescence in H2B-GFP^{-} HSCs was significantly lower in *Nras*$^{G12D/+}$ as compared to control mice (Extended data Figure 6b), suggesting that H2B-GFP^{-} *Nras*$^{G12D/+}$ HSCs underwent more rounds of division on average. In contrast, the median level of GFP fluorescence in H2B-GFP^{hi} HSCs was significantly higher in *Nras*$^{G12D/+}$ as compared to control mice (Extended data Figure 6b), suggesting that H2B-GFP^{hi} *Nras*$^{G12D/+}$ HSCs tended to divide less than control H2B-GFP^{hi} HSCs on average. *Nras*$^{G12D/+}$ thus had a bimodal effect, increasing the division of some HSCs and reducing the division of other HSCs.

We followed another cohort of age and sex-matched pairs of *Mx1-cre; Nras*$^{G12D/+}$ and control mice for 15 weeks after doxycycline removal. In five independent experiments, *Nras*^{G12D} significantly increased the frequency of H2B-GFP^{hi} HSCs in every pair of mice we examined (n=7; $p<0.05$) (Figure 3c). We observed increased frequencies of H2B-GFP^{-} HSCs in the *Nras*$^{G12D/+}$ mice from some pairs but not others, and overall the effect was not statistically significant (Figure 3c). Since the rapidly dividing subset of *Nras*$^{G12D/+}$ HSCs differentiates more quickly than control HSCs (Figure 3d), prolonged periods of chase after H2B-GFP labeling may not be appropriate to quantify the frequency of these cells.

Nras$^{G12D/+}$ significantly increased the rate at which MPPs divided (Extended data Figure 6c).

To test the relationship between division history and competitiveness we transplanted 15 CD150^{+}CD48^{-}LSK H2B-GFP^{hi} HSCs, 50 H2B-GFP^{lo} moderately cycling HSCs, or 75 H2B-GFP^{-} frequently cycling HSCs from *Nras*$^{G12D/+}$ or control donor mice after 12 weeks of chase into irradiated wild-type recipients along with 3×10^{5} recipient bone marrow cells. The *Nras*$^{G12D/+}$ H2B-GFP^{-} frequently cycling HSCs gave significantly lower levels of donor cell reconstitution, at least in the myeloid lineages, as compared to control H2B-GFP^{-} HSCs (Figure 3d). In contrast, the *Nras*$^{G12D/+}$ H2B-GFP^{lo} and H2B-GFP^{hi} HSCs gave significantly ($p<0.05$) higher levels of donor cell reconstitution in all lineages than the control H2B-GFP^{lo} and H2B-GFP^{hi} HSCs (Figure 3d). *Nras*$^{G12D/+}$ thus reduced the division and increased the competitiveness of some HSCs while increasing the division and reducing the competitiveness of other HSCs.

We continuously administered BrdU to *Mx1-cre; Nras*$^{G12D/+}$ versus control mice beginning two weeks after pIpC treatment. We assessed the frequency of BrdU+ HSCs after 4, 10, 20, and 30 days of BrdU treatment (Extended data Figure 6d). Relative to control HSCs, significantly more *Mx1-cre; Nras*$^{G12D/+}$ HSCs incorporated BrdU after 4 (32±0.1% versus 24±1.2%, $p<0.01$) and 10 (64±5.9% versus 45±3.6%, $p<0.02$) days of BrdU administration. In contrast, significantly fewer *Mx1-cre; Nras*$^{G12D/+}$ HSCs incorporated BrdU after 20 (78±4.7% versus 86±0.7%, $p<0.05$) and 30 (86±3.4% versus 92±4.8%, $p<0.02$) days of BrdU administration. These data are consistent with the H2B-GFP label retention data in demonstrating that some *Nras*$^{G12D/+}$ HSCs divide more frequently while other *Nras*$^{G12D/+}$ HSCs divide less frequently than control HSCs.

We detected the activation of the canonical Ras effector, ERK, in bone marrow cells from *Mx1-cre; Nras*$^{G12D/+}$ and *Mx1-cre; Nras*$^{G12D/G12D}$ mice but not in LSK stem/progenitor cells or Lineage^{-}c-kit^{+}Sca-1^{-} myeloid progenitors (Extended data Figure 8a). We treated *Mx1-cre; Nras*$^{G12D/+}$ or control mice with the MEK inhibitors, PD0325901 (5mg/kg/day) or AZD6244 (25mg/kg/day), and assessed the effects on BrdU incorporation in CD150^{+}CD48^{-}LSK HSCs. After eight days of treatment, splenocytes from PD0325901-treated mice of both genotypes showed reduced pERK levels (Extended data Figure 8b), but this did not affect the increased rate of BrdU incorporation by *Nras*$^{G12D/+}$ HSCs (Extended data Figure 8c). In contrast, when we performed the same experiments with AZD6244, pERK activation was completely blocked in bone marrow and spleen (Extended data Figure 8d) and the increased cycling of *Nras*$^{G12D/+}$ HSCs was abolished (Supplementary figure 8e). These data suggest that the more stringent inhibition of pERK activation by AZD6244 blocks the effect of *Nras*$^{G12D/+}$ on HSC cycling.

We did not detect increased Akt (Extended data Figure 8f), S6, or p38 (Figure 4a) phosphorylation in whole bone marrow cells, CD48^{-}LSK cells (HSCs and MPPs) or CD48^{+}LSK cells (mainly restricted progenitors[22]) from *Mx1-cre; Nras*$^{G12D/+}$ mice.

We performed gene expression profiling of H2B-GFP^{-} and H2B-GFP^{hi} CD150^{+}CD48^{-}LSK HSCs from 3 pairs of *Mx1-cre; Nras*$^{G12D/+}$; *Col1A1-H2B-GFP; Rosa26-M2-rtTA* mice and

littermate controls 12 weeks after removal of doxycycline. Gene set enrichment analysis (GSEA) revealed that cell cycle genes were significantly enriched in H2B-GFP^{-} *Nras*$^{G12D/+}$ HSCs as compared to H2B-GFP^{-} control HSCs ($p<0.0001$) but not in H2B-GFP^{hi} *Nras*$^{G12D/+}$ HSCs as compared to H2B-GFP^{hi} control HSCs (Extended data Figure 7d). DNA replication genes and RNA polymerase genes were significantly enriched in H2B-GFP^{-} *Nras*$^{G12D/+}$ HSCs as compared to H2B-GFP^{-} control HSCs ($p<0.05$) but were significantly depleted in H2B-GFP^{hi} *Nras*$^{G12D/+}$ HSCs as compared to H2B-GFP^{hi} control HSCs ($p<0.01$; Extended data Figure 7e, 7f). These data demonstrate different transcriptional responses to Nras activation in H2B-GFP^{-} as compared to H2B-GFP^{hi} HSCs: genes associated with cell cycling were induced by Nras activation in the H2B-GFP^{-} HSCs but repressed by Nras activation in the H2B-GFP^{hi} HSCs.

Only two genes showed a similar change in expression with Nras activation in all of the multipotent cells we studied ($p\leq0.05$ and fold change≥2; Extended data Figure 7a–c). One of these, *Suppressor of cytokine signaling 2* (*Socs2*), was significantly reduced in expression in *Nras*$^{G12D/+}$ as compared to control cells by microarray and qRT-PCR (Extended data Figure 7c and 8g–i). SOCS2 negatively regulates STAT signaling in hematopoietic cells [23,24]. We observed an increase in phosphorylated STAT5, but not STAT3, levels in *Nras*$^{G12D/+}$ as compared to control CD48^{-}LSK cells, without affecting total STAT5 levels (Figure 4a, 4b, and Extended data Figure 8j).

To test whether the increased STAT5 phosphorylation in *Nras*$^{G12D/+}$ CD48^{-}LSK cells increased HSC proliferation and self-renewal we mated *Stat5ab*$^{fl/+}$ mice [25] with *Mx1-cre; Nras*$^{G12D/+}$ mice. Two weeks after finishing pIpC treatment, western blot of sorted CD48^{-}LSK cells confirmed that deletion of one allele of *Stat5ab* in *Nras*$^{G12D/+}$ HSCs reduced the levels of pSTAT5 and total STAT5 (Extended data Figure 8k). *Stat5ab*$^{-/+}$ HSCs exhibited normal BrdU incorporation and *Nras*$^{G12D/+}$ HSCs exhibited increased proliferation relative to control HSCs (Figure 4c). Deletion of one allele of *Stat5ab* in *Nras*$^{G12D/+}$ HSCs significantly reduced the rate of BrdU incorporation ($p<0.05$). A reduction in STAT5 levels thus rescued the effects of Nras^{G12D} on HSC cycling. Neither deletion of *Stat5ab* nor activation of *Nras*$^{G12D/+}$ significantly affected BrdU incorporation by the myeloid progenitors we examined (Extended data Figure 8l).

We next transplanted 5×10^5 whole bone marrow cells from control, *Mx-1-Cre; Nras*$^{G12D/+}$ (*NrasG12D*/+), *Mx-1-Cre; Stat5a/b*$^{-/+}$ (*Stat5ab*−/+), or *Mx-1-Cre; Nras*$^{G12D/+}$; *Stat5a/b*$^{-/+}$ (double mutant) donors (2 weeks after finishing pIpC treatment) into irradiated wild-type recipients along with 5×10^5 recipient bone marrow cells. *Nras*$^{G12D/+}$ cells gave significantly higher levels of reconstitution than control cells in all lineages for at least 20 weeks after transplantation (Figure 4d). Loss of one *Stat5ab* allele (*Stat5ab*+/−) reduced the level of reconstitution by donor cells relative to control cells but the difference was not statistically significant. In contrast, loss of a single allele of *Stat5ab* in the *Nras*$^{G12D/+}$ background completely blocked the increased reconstitution by *Nras*$^{G12D/+}$ cells such that levels of donor cell reconstitution were indistinguishable from control cells (Figure 4d). An increase in STAT5 signaling is therefore required for increased competitiveness by *Nras*^{G12D} HSCs.

Nras^{G12D} is likely an early mutation in some leukemias as it is widely observed in both MPN and myeloid leukemias[2] and *Nras*^{G12D} mutations in mice lead only to a late onset MPN with prolonged survival[16,17]. *NRAS* and *KRAS* mutations are frequently among the first mutations observed in pre-leukemic clones that precede CMML[26]. Some JMML patients undergo remission, with or without therapy, yet continue to carry *NRAS* mutations in their hematopoietic cells[27,28]. Germline *NRAS* mutations have also been reported in JMML patients [29], or patients with Noonan syndrome that develop JMML[30]. The evidence that *NRAS* mutations can be found in normal hematopoietic cells, despite predisposing for the development of neoplasms, is consistent with our conclusion that they promote pre-leukemic clonal expansion.

Our data provide a molecular explanation for how pre-leukemic clonal expansion may occur. *Nras*$^{G12D/+}$ has a bimodal effect on HSCs, increasing self-renewal potential and reducing division in one subset of HSCs while increasing division and reducing self-renewal in another subset of HSCs. Short-lived but rapidly dividing *Nras*$^{G12D/+}$ HSCs presumably outcompete wild-type HSCs and are replenished over time by quiescent *Nras*$^{G12D/+}$ HSCs that are slowly recruited into cycle. It will be interesting to determine whether the ability to induce bimodal responses in stem cell pools is a common feature of mutations that promote pre-malignant clonal expansion.

EXTENDED DATA

METHODS

Mice—All mice were housed in the Unit for Laboratory Animal Medicine at the University of Michigan and protocols were approved by the University of Michigan Committee on the Use and Care of Animals. *Nras*$^{G12D/+}$ [20], *Stat5ab*$^{+/-}$ [25], *Col1A1-H2B-GFP; Rosa26-M2-rtTA*[4], *Vav1-Cre*, and *Mx-1-Cre* mice were backcrossed for at least 10 generations onto a C57BL/Ka-CD45.2:Thy-1.1 background. Recipients in reconstitution assays were adult C57BL/Ka-CD45.1:Thy-1.2 mice, at least 8 weeks old at the time of irradiation. pIpC (Amersham) was reconstituted in PBS and administered at 0.5 μg/gram body mass/day by intraperitoneal injection. BrdU (Sigma) was administered as a single dose of 200mg/kg body mass by intraperitoneal injection followed by 1mg/ml BrdU in the drinking water. For long term BrdU administration, BrdU water was changed every 3 days. Doxycycline (Research Products International Corporation) was added to the water at a concentration of 0.2% (m/v) along with 1% sucrose (Fisher).

Statistical Methods—Multiple independent experiments were performed to verify the reproducibility of all experimental findings. Group data always represents mean±standard deviation. Unless otherwise indicated, two-tailed Student's t-tests were used to assess statistical significance. No randomization or blinding was used in any experiments. Experimental mice were not excluded in any experiments. In the case of measurements in which variation among experiments tends to be low (e.g. HSC frequency) we generally examined 3–6 mice. In the case of measurements in which variation among experiments tends to be higher (e.g. reconstitution assays) we examined larger numbers of mice (7–20).

PCR of genomic DNA for genotyping—To assess the degree of *Nras*^{G12D} recombination in HSCs from *Mx1-cre; Nras*$^{G12D/+}$ mice after pIpC treatment, bone marrow cells were harvested and stained for surface markers as described above. Single HSCs ($CD150^+CD48^-$LSK cells) were sorted into 96 well plates containing methylcellulose medium (M3434, Stem Cell Technologies) and incubated for 14 days at 37°C. Cells from each colony were re-suspended in PBS then incubated with alkaline lysis buffer (25 mM NaOH, 0.2 mM EDTA), boiled, then neutralized by addition of an equal volume of neutralizing buffer (40 mM Tris-HCl). The neutralized extract was used for PCR with the following primers: F2: 5' - aga cgc gga gac ttg gcg agc - 3'; R1: 5' - gct gga tcg tca agg cgc ttt tcc - 3'. To genotype mouse tail DNA for the presence of the *Nras*^{G12D} allele, primers R1 and F2 were used in addition to primer SD5', 5' - agc tag cca cca tgg ctt gag taa gtc tgc a - 3'. To genotype for the presence of the *Mx1-cre* transgene, primers F1 and R1 were used: F1 5'-att gct gtc act tgg tcg tgg c-3', R1 5'-gaa aat gct tct gtc cgt ttg c-3'. To check the presence of the *Rosa26-M2-rtTA* transgene, the following primers were used: 5' Aaa gtc gct ctg agt tgt tat 3'; 5' Gcg aag agt ttg tcc tca acc 3'; and 5' Gga gcg gga gaa atg gat atg 3'. To genotype mice for the presence of the *Col1A1-H2B-GFP* transgene, the following primers were used: 5' ctg aag ttc atc tgc acc acc 3', 5' gaa gtt gta ctc cag ctt gtg c 3'. To genotype mice for the deletion of *Stat5ab*, the following primers were used: 5' gaa agc agc atg aaa ggg ttg gag 3'; 5' agc agc aac cag agg act ac 3'; and 5' aag tta tct cga gtt agt cag g 3'.

Flow cytometry and HSC isolation—Bone marrow cells were flushed from the long bones (tibias and femurs) with Hank's buffered salt solution without calcium or magnesium, supplemented with 2% heat-inactivated calf serum (HBSS; Invitrogen). Cells were triturated and filtered through nylon screen (70 mm; Sefar America) to obtain a single-cell suspension. $CD150^+CD48^-Lin^-Sca1^+c\text{-}kit^+$ HSCs and $CD150^-CD48^-Lin^-Sca1^+c\text{-}kit^+$ MPPs were isolated as previously described[21,22]. For isolation of HSCs, whole bone marrow cells were incubated with antibodies to lineage (Lin) markers including B220 (6B2), CD3 (KT31.1), CD5 (53-7.3), CD8 (53-6.7), Gr-1 (8C5), CD41 (MWReg30) and Ter119 (Ter-119) that were conjugated to FITC, anti-CD150 antibody (TC15-12F12.2) conjugated to PE, anti-CD48 antibody (HM48-1) conjugated to PE-Cy7, anti-c-kit antibody (2B8) conjugated to APC, and anti-Sca1 antibody (D7) conjugated to PerCP/Cy5.5 (all antibodies were purchased from Biolegend). After washing, cells were incubated with anti-APC conjugated to paramagnetic microbeads (Miltenyi Biotec). The microbead bound ($c\text{-}kit^+$) cells were then enriched using LS columns (Miltenyi Biotec). To identify $CD45.2^+$ HSCs, antibodies against CD45.2 (104-FITC; BioLegend) and CD45.1 (A20-APC780, BioLegend) were used. Non-viable cells were excluded from sorts and analyses using the viability dye 4′,6-diamidino-2-phenylindole (DAPI) (1 μg/ml). BrdU incorporation *in vivo* was measured by flow cytometry using the APC BrdU Flow Kit (BD Biosciences). To perform Pyronin Y and DAPI staining, $CD150^+CD48^-$LSK HSCs were sorted into 100% Ethanol and placed in the cold room overnight. The cells were then washed with PBS and stained with Pyronin Y (1ug/ml) and DAPI (10ug/ml) for 30 minutes before flow cytometric analysis

Long-term competitive repopulation assay—Adult recipient mice (CD45.1) were irradiated with an Orthovoltage X-ray source delivering approximately 300 rad min^{-1} in two equal doses of 540 rad, delivered at least 2 h apart. Cells were injected into the retro-orbital

venous sinus of anaesthetized recipients. Beginning 4 weeks after transplantation and continuing for at least 16 weeks, blood was obtained from the tail veins of recipient mice, subjected to ammonium-chloride potassium red cell lysis, and stained with directly conjugated antibodies to CD45.2 (104), CD45.1 (A20), B220 (6B2), Mac-1 (M1/70), CD3 (KT31.1) and Gr-1 (8C5) to monitor engraftment.

BrdU incorporation by myeloid progenitors—Two and a half hours after BrdU administration, whole bone marrow cells were incubated first with anti-ckit antibody conjugated to biotin (2B8) then with antibodies to lineage (Lin) markers including B220 (6B2), CD3 (KT31.1), CD5 (53-7.3), CD8 (53-6.7), Gr-1 (8C5), CD41 (MWReg30) and Ter119 (Ter-119) that were conjugated to phycoerythrin (PE), anti-CD34 antibody (eBioscience, RAM34) conjugated to FITC, anti-CD16/CD32 antibody (93) conjugated to PE-Cy7, streptavidin conjugated to Alexa700 (Invitrogen S21383), and anti-Sca1 antibody (D7) conjugated to PerCP/Cy5.5 (all antibodies were purchased from Biolegend unless otherwise stated). BrdU incorporation was measured by flow cytometry using the APC BrdU Flow Kit (BD Biosciences).

Western blotting—The same number of cells (30,000 cells for $CD48^{-}$LSK cells or CD48+LSK cells; 100,000 cells for LSK or $Lineage^{-}ckit^{+}Sca\text{-}1^{-}$ cells) from each population to be analysed were sorted into HBSS with 2% FCS. The cells were then washed and incubated with 100ng/ml TPO and 100ng/ml SCF at 37°C for 30 minutes. The cells then were washed with PBS and precipitated with trichloroacetic acid (TCA) at a final concentration of 10% TCA. Extracts were incubated on ice for 15 min and spun down for 10 min at 16,100*g* at 4 °C. The supernatant was removed and the pellets were washed with acetone twice then dried. The protein pellets were solubilized with solubilization buffer (9 M urea, 2% Triton X-100, 1% DTT) before adding LDS loading buffer (Invitrogen). Proteins were separated on a Bis-Tris polyacrylamide gel (Invitrogen) and transferred to a PVDF membrane (Millipore). All antibodies were purchased from Cell Signaling technology. These include anti-pERK (T202/Y204), anti-pAkt (T308), anti-pS6 (S240/244), anti-pStat5 (Y694), anti-Stat3 (Y705), anti-ERK (137F5), anti-Stat5 (3H7), anti-pp38 (T180/Y182) and anti-β-actin (8H10D10).

Gene expression profiling—$CD150^{+}CD48^{-}$LSK HSCs and $CD150^{-}CD48^{-}$LSK MPPs were isolated by flow cytometry. Total RNA was isolated using Trizol (Invitrogen) followed by Qiagen RNeasy Micro kit purification according to the manufacturer's protocols. For microarray analysis, reverse transcription and linear amplification was performed on total RNA using the NuGen Ovation pico WTA system version 2 and then purified with the Qiaquick PCR purification kit (Qiagen). Six micrograms of amplified cDNAs were labeled with biotin using the Encore Biotin Module (NuGen) and submitted to the Microarray Core Facility of the University of Michigan Comprehensive Cancer Center for hybridization to Affymetrix Mouse Genome 430 2.0 Arrays. Statistical analyses were performed using R[33] version 2.15.2 and Bioconductor version 2.11[34]. Gene expression signals were normalized to the trimmed average of 500 using the Affymetrix MAS 5.0 algorithm. MAS5 signals less than 2 were set to 2 before log2 transformation. Probe sets with MAS5 absent calls for all samples were excluded. Differential expression analysis was performed by limma[35] with

estimation of fold change. Probe sets with limma p-value<0.05 and fold change>2 were considered differentially expressed. Gene Set Enrichment Analysis[36] was used to assess pathway enrichment. Gene expression data have been deposited to the Gene Expression Omnibus (http://www.ncbi.nlm.nih.gov/geo/; accession number GSE45194).

Quantitative RT-PCR—Total RNA was collected as described above and reverse transcription was performed with the High Capacity cDNA reverse transcription kit (Applied Biosystems). Real time PCR was performed with Absolute Sybr Green Rox mix (Thermo Scientific) using an ABI 7300 PCR machine. RNA from 100 cells was used for each reaction. Transcript levels were normalized to β-*actin*.

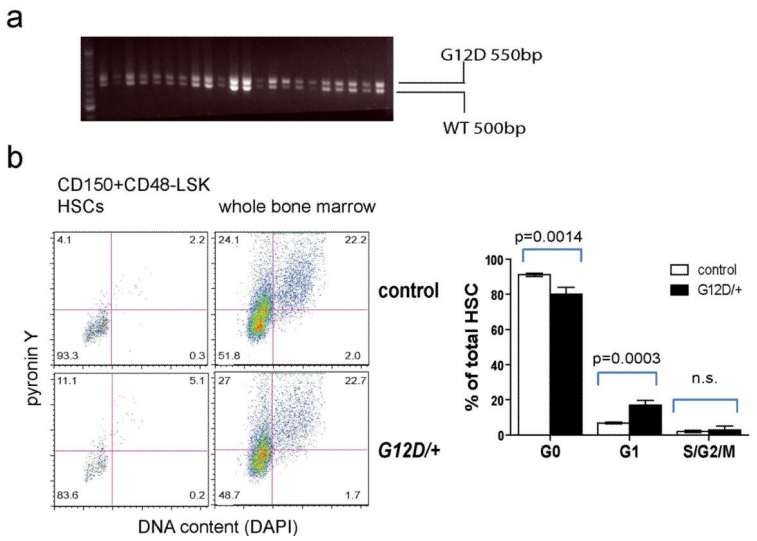

Extended data Figure 1.

a) The *Nras*^{G12D} allele was recombined in all HSCs after 3 doses (every other day) of pIpC. Two weeks after the last dose of pIpC was administered to *Mx1-cre; Nras*$^{G12D/+}$ mice, the mice were sacrificed and individual CD150^{+}CD48^{-}LSK HSCs were sorted into methylcellulose cultures in 96 well plates. The cells were cultured for 14 days then DNA was extracted from individual colonies and genotyped by PCR. The size of the recombined *Nras*^{G12D} allele (G12D) was 550bp and the *Nras*$^{+}$ allele (WT) was 500bp. *Nras* recombination was observed in 22 of 22 HSC colonies examined. Blot is representative of three independent experiments. **b**) Cell cycle analysis of HSCs by pyronin Y and DAPI staining. CD150^{+}CD48^{-}LSK HSCs were sorted from *Mx1-cre; Nras*$^{G12D/+}$ mice and littermate controls into 100% ethanol and stained with pyronin Y and DAPI to identify cells in G0 (left lower quadrant), G1 (left upper quadrant) and S/G2/M (right upper and lower quadrants). Data represent mean±s.d.. Statistical analysis was performed with a two-way ANOVA (P<0.01, n=4) followed by pairwise posthoc t-tests.

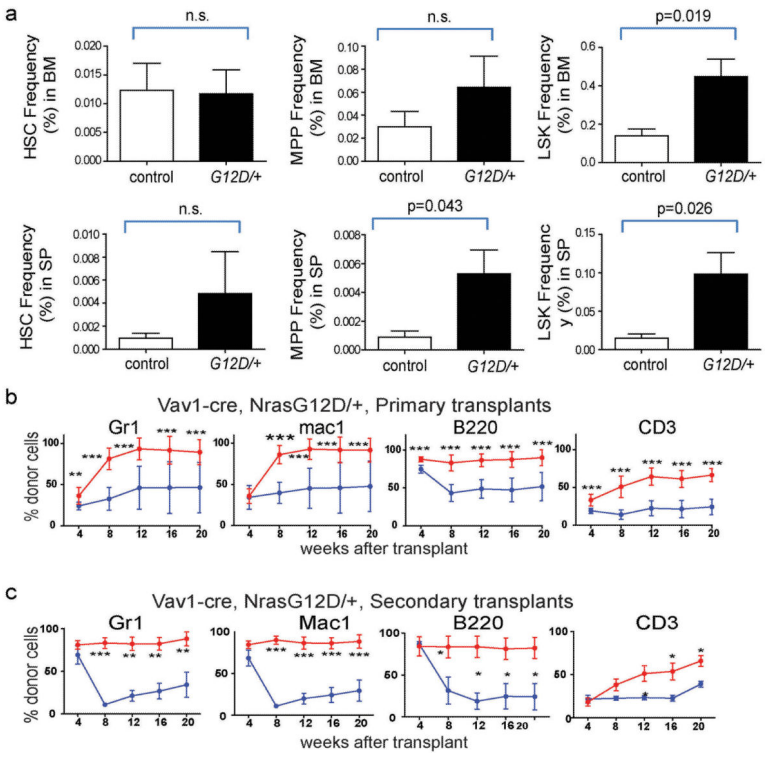

Extended data Figure 2. HSC competitiveness is increased in *Vav1-Cre; Nras$^{G12D/+}$* mice

a) Frequencies of CD150^{+}CD48^{-}LSK HSCs, CD150^{-}CD48^{-}LSK MPPs, and LSK cells in the bone marrow (BM, top row) and spleen (sp, bottom row) of *Vav1-cre; Nras$^{G12D/+}$* (G12D/+) or littermate control (con) mice (n=4) at 6-10 weeks of age. **b**) 5×10^{5} donor bone marrow cells from *Vav1-cre; Nras$^{G12D/+}$* (G12D/+) or littermate control (con) mice at 6-10 weeks of age were transplanted into irradiated recipient mice along with 5×10^{5} recipient bone marrow cells (3 donors/genotype were each transplanted into 4 recipients/donor). **c**) Secondary transplantation of 3×10^{6} bone marrow cells from primary recipient mice in Extended data Figure 2b at 20 weeks after transplantation (2 primary recipients/genotype were each transplanted into 4 secondary recipients/primary recipient). Data represent mean ±s.d.. Two-tailed student's t-tests were used to assess statistical significance. *P<0.05, **P<0.01, ***P<0.001.

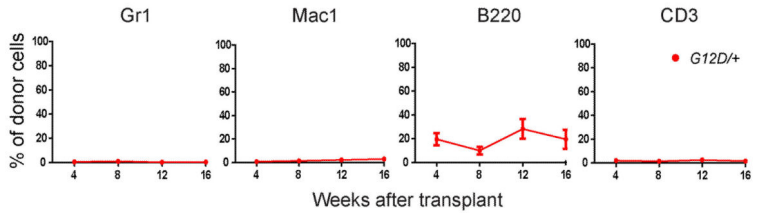

Extended data Figure 3. HSCs from *Mx1-cre; Nras$^{G12D/+}$* mice were not immortalized

A fifth round of serial transplantation of 3×10^{6} bone marrow cells from the quaternary recipients of *Nras$^{G12D/+}$* (G12D/+) bone marrow cells shown in Figure 2c showed that the *Nras$^{G12D/+}$* HSCs eventually exhausted all of their HSCs and MPPs and were able to only

give low levels of lymphoid reconstitution. Four donor mice from Figure 2c were transplanted 20 weeks after the fourth round of transplantation into 4 recipients per quaternary donor. The data represent mean±s.d. for donor blood cells in the myeloid (Gr-1$^+$ or Mac-1$^+$ cells), B (B220$^+$), and T (CD3$^+$) cell lineages.

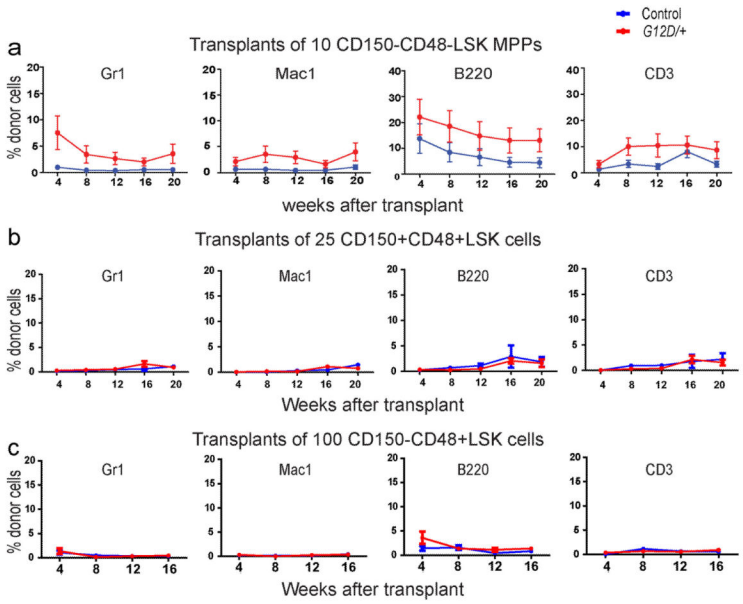

Extended data Figure 4. *Nras*^{G12D} (G12D/+) expression increased the reconstituting potential of CD150$^-$CD48$^+$LSK MPPs but did not affect the reconstituting potential of CD150$^+$CD48$^+$LSK, or CD150$^-$CD48$^+$LSK progenitors in irradiated mice

a) 10 donor MPPs, **b)** 25 CD150$^+$CD48$^+$LSK progenitors, or **c)** 100 CD150$^-$CD48$^+$LSK progenitors from *Mx1-cre; Nras*$^{G12D/+}$ (G12D/+) or littermate control (con) mice at 2 weeks after pIpC treatment were transplanted into irradiated recipient mice along with 3×10^5 recipient bone marrow cells. Data represent mean±s.d. for donor blood cells in the myeloid (Gr-1$^+$ or Mac-1$^+$ cells), B (B220$^+$), and T (CD3$^+$) cell lineages. Two-tailed student's t-tests were used to assess statistical significance. None of the time points were significantly different between treatments. The data represent two independent experiments with 4 recipient mice per donor

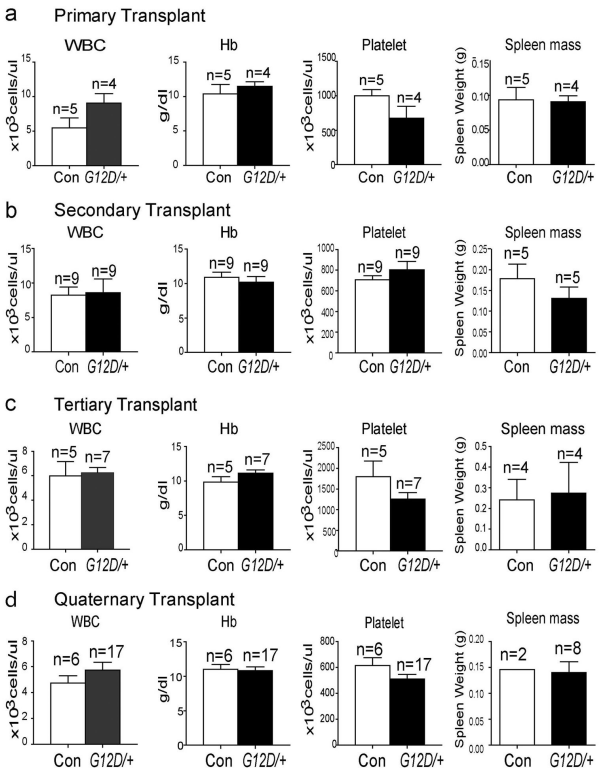

Extended data Figure 5. *Nras*^{G12D}-induced changes in HSC function were not associated with the development of leukemia

White blood counts (WBC), hemoglobulin (Hb) levels, platelet counts, and spleen masses for recipient mice from primary transplants (**a**; from Figure 1d), secondary transplants (**b**; from Figure 2a), tertiary transplants (**c**; from Figure 2b) and quaternary transplants (**d**; from Figure 2c). In all cases, these blood cell counts were collected from mice after the analysis of blood cell reconstitution was complete (at least 20 weeks after transplantation). The transplanted mice were observed for a median time of 260 (162–315) days for primary recipient mice, 194 (122–264) days for secondary recipient mice, 224 (176–336) days for tertiary recipient mice, and 280 (279–280) days for quaternary recipient mice. We never observed evidence of leukemia or MPN by histology in these mice. Across all of the experiments, only two recipients of *Nras*$^{G12D/+}$ cells and two recipients of control cells died spontaneously. Data represent mean±s.d.. Two-tailed student's t-tests were used to assess statistical significance and none of the comparisons showed significant difference.

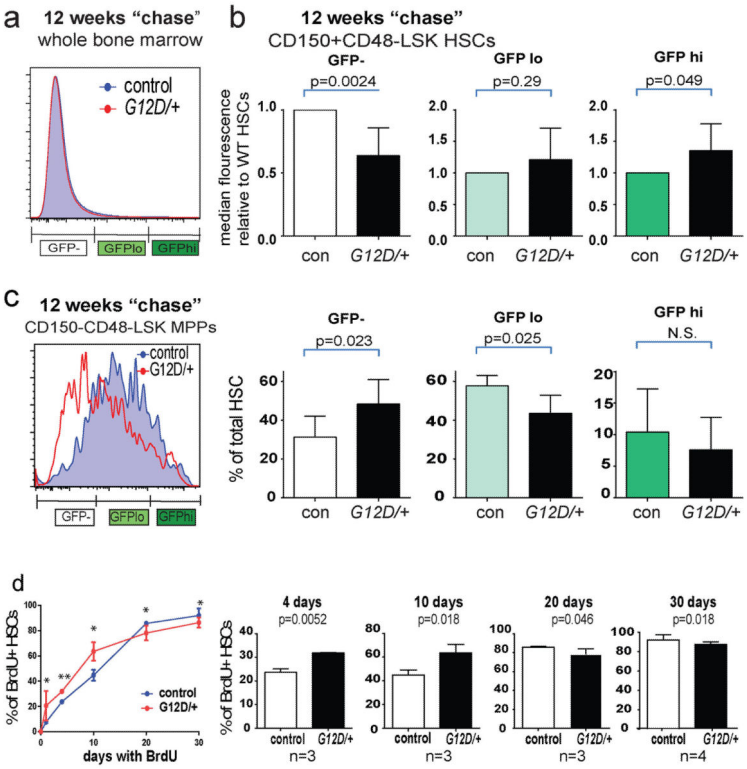

Extended data Figure 6. *Nras*$^{G12D/+}$ had a bimodal effect on HSC cycling but increased the rate at which MPPs divide

a) Flow cytometric analysis of GFP expression in whole bone marrow cells from *Nras*$^{G12D/+}$ or littermate control mice after 12 weeks of chase without doxycycline. **b)** Median GFP fluorescence intensity of H2B-GFP^{-}, H2B-GFP^{lo} and H2B-GFP^{hi} HSCs from wild type and *Nras*$^{G12D/+}$ mice (n=8 mice/genotype). GFP levels in control HSCs were set to one for comparison to relative levels in *Nras*$^{G12D/+}$ HSCs. **c)** Nras^{G12D} increased the rate of division by MPPs. Flow cytometric analysis of GFP expression in CD150^{-}CD48^{-}LSK MPPs from *Mx1-cre; Nras*$^{G12D/+}$; *Col1A1-H2B-GFP; Rosa26-M2-rtTA* mice (G12D/+) and littermate controls (con) after 12 weeks of chase(n=8 mice/genotype). Relative to control MPPs, *Nras*$^{G12D/+}$ MPPs included significantly more H2B-GFP^{-} frequently cycling cells and significantly fewer H2B-GFP^{lo} MPPs ($p<0.05$ by two-way ANOVA and posthoc pairwise t-tests). **d**) We continuously administered BrdU to *Mx1-cre; Nras*$^{G12D/+}$ versus control mice for 1 to 30 days and determined the frequency of BrdU+ HSCs (1 day BrdU data are from Figure 1a). Data represent mean±s.d.. Two-tailed student's t-tests were used to assess statistical significance unless stated otherwise. *P<0.05, **P<0.01, ***P<0.001.

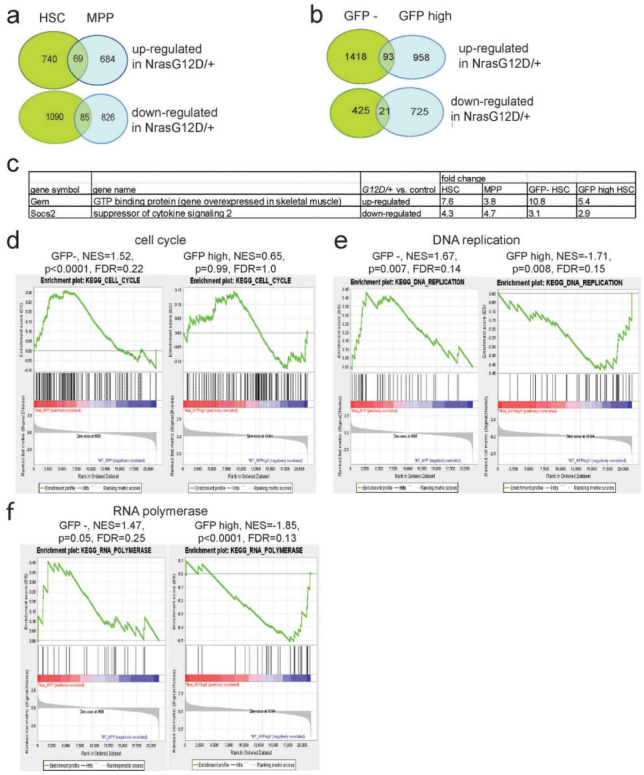

Extended data Figure 7. Gene expression profiling demonstrates different transcriptional responses to Nras activation in quiescent as compared to frequently dividing HSCs

a) $CD150^{+}CD48^{-}LSK$ HSCs and $CD150^{-}CD48^{-}LSK$ MPPs were isolated from three pairs of *Mx1-cre; Nras*$^{G12D/+}$ and littermate controls and gene expression profiling was performed with Affymetrix mouse genome 430 2.0 microarrays. The Venn diagram shows the number of genes that were differentially expressed between *Nras*$^{G12D/+}$ and controls cells within each cell population (fold change≥2). **b**) Venn diagram of genes that were differentially expressed between *Nras*$^{G12D/+}$ and control GFP^{-} HSCs and GFP^{high} HSCs isolated from 3 pairs of *Mx1-cre*; *Nras*$^{G12D/+}$; *Col1A1-H2B-GFP; Rosa26-M2-rtTA* mice and littermate controls (fold change ≥and p value ≤0.05). **c**) Genes that were consistently increased or decreased in expression in response to Nras activation in HSCs, MPPs, GFP^{-} HSCs, and GFP^{high} HSCs (fold change≥2 and p≤0.05 in each cell population). **d, e, f**) Gene set enrichment analysis (GSEA) of cell cycle genes **d**), DNA replication genes **e**) and RNA polymerase genes **f**).

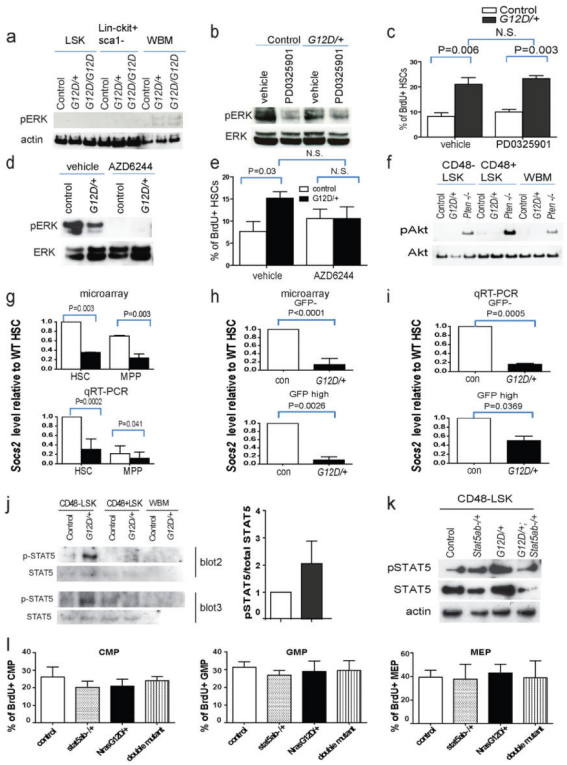

Extended data Figure 8. Nras activation increases STAT5 phosphorylation

a) Western blot for phosphorylated ERK (pERK) in LSK stem/progenitor cells, Lin^{-}c-kit^{+}Sca1^{-} progenitor cells, or whole bone marrow (WBM) cells from *Mx1-cre; Nras*$^{G12D/+}$ (G12D/+) mice, *Mx1-cre; Nras*$^{G12D/G12D}$ (G12D/G12D) mice, or littermate controls 2 weeks after pIpC treatment **b**) Western blot of pERK and total ERK in 10^{6} uncultured splenocytes from *Mx1-cre; Nras*$^{G12D/+}$ (G12D/+) or control mice after 8 days treatment with PD0325901 MEK inhibitor or vehicle (blot is representative of four independent experiments). **c**) The frequency of BrdU^{+} CD150^{+}CD48^{-}LSK HSCs after a 24-hour pulse of BrdU to *Mx1-cre; Nras*$^{G12D/+}$ (G12D/+) or control mice after 7 days of PD0325901 MEK inhibitor or vehicle (mean±s.d. from four experiments). **d**) Western blot of pERK and total ERK in 10^{6} uncultured bone marrow cells from *Mx1-cre; Nras*$^{G12D/+}$ (G12D/+) or control mice after 8 days of AZD6244 MEK inhibitor or vehicle (blot is representative of four independent experiments). **e**) The frequency of BrdU^{+} CD150^{+}CD48^{-}LSK HSCs after a 24-hour pulse of BrdU to *Mx1-cre; Nras*$^{G12D/+}$ (G12D/+) or control mice after 7 days of AZD6244 MEK inhibitor or vehicle (mean±s.d. from four experiments). **f**) Western blot for phosphorylated Akt (pAkt) in CD48^{-}LSK HSCs/MPPs, CD48^{+}LSK progenitors, or WBM cells from *Mx1-cre; Nras*$^{G12D/+}$ (G12D/+) mice, *Mx1-cre; Pten*$^{fl/fl}$ (*Pten*$^{-/-}$) mice, or littermate controls 2 weeks after pIpC treatment. **g**) *Socs2* transcript levels in HSCs and MPPs from *Mx1-cre; Nras*$^{G12D/+}$ (G12D/+) or control mice by microarray analysis (top, n=3) and qRT-PCR (bottom, n=7). **h, i**) *Socs2* transcript levels in GFP^{-} and GFP^{high} HSCs from *Mx1-cre; Nras*$^{G12D/+}$; *Col1A1-H2B-GFP; Rosa26-M2-rtTA* mice and littermate controls by microarray (**h**, n=3) and qRT-PCR (, n=3). **j**) Western blotting showed that pSTAT5 levels were significantly increased in CD48^{-}LSK HSCs/MPPs from *Mx1-cre;*

Nras$^{G12D/+}$ mice as compared to control mice. Left panel shows western blots of pSTAT5 and total STAT5 from two independent experiments. Right panel shows quantification of pSTAT5 levels from western blots from three independent experiments (signals were quantitated using NIH ImageJ software). Blot 1 was shown in Figure 4e. k) Western blot showed that STAT5 levels were reduced in CD48^{-}LSK HSCs/MPPs from *Mx1-cre; Stat5ab*$^{-/+}$ or *Mx1-cre; Nras*$^{G12D/+}$; *Stat5ab*$^{-/+}$ mice as compared to control and *Mx1-cre; Nras*$^{G12D/+}$ mice (blot is representative of four independent experiments). **l**) BrdU incorporation into common myeloid progenitors (CMPs; Lin^{-}Sca1^{-}ckit^{+}CD34^{+}CD16/32^{-}), granulocyte macrophage progenitors (GMPs; Lin^{-}Sca1^{-}ckit^{+}CD34^{+}CD16/32^{+}), and megakaryocyte erythroid progenitors (MEPs; Lin^{-}Sca1^{-}ckit^{+}CD34^{-}CD16/32^{-}) from control, *Mx1-cre; Stat5ab*$^{-/+}$, *Mx1-cre; Nras*$^{G12D/+}$, or *Mx1-cre; Nras*$^{G12D/+}$; *Stat5ab*$^{-/+}$ mice after a 2.5 hour pulse of BrdU (n=4 mice/treatment). Data represent mean±s.d.. Two-tailed student's t-tests were used to assess statistical significance.

EXTENDED DATA REFERENCES

31. Yilmaz OH, et al. Pten dependence distinguishes haematopoietic stem cells from leukaemia-initiating cells. Nature. 2006; 441:475–482. [PubMed: 16598206]
32. Lee JY, et al. mTOR activation induces tumor suppressors that inhibit leukemogenesis and deplete hematopoietic stem cells after Pten deletion. Cell stem cell. 2010; 7:593–605. [PubMed: 21040901]
33. R Development Core Team. R: A language and environment for statistical computing. 2009. http://www.R-project.org
34. Gentleman RC, et al. Bioconductor: open software development for computational biology and bioinformatics. Genome Biol. 2004; 5:R80. [PubMed: 15461798]
35. Smyth GK. Linear models and empirical bayes methods for assessing differential expression in microarray experiments. Stat Appl Genet Mol Biol. 2004; 3 Article3.
36. Subramanian A, et al. Gene set enrichment analysis: a knowledge-based approach for interpreting genome-wide expression profiles. Proceedings of the National Academy of Sciences of the United States of America. 2005; 102:15545–15550. [PubMed: 16199517]

ACKNOWLEDGEMENTS

SJM is a Howard Hughes Medical Institute Investigator and the Mary McDermott Cook Chair in Pediatric Genetics. This work was supported by the Cancer Prevention and Research Institute of Texas. Q.L. was supported by NIH K08-CA-134649 and V Foundation V Scholar award. Thanks to Drs. Lothar Hennighausen, Kevin Haigis, and Hanno Hock for generously providing *Stat5ab*^{fl}, *Nras*^{G12D}, and *Col1A1-H2B-GFP; Rosa26-M2-rtTA* mice. Thanks to Maggie Heeren and Kritika Rajan for help with genotyping and to Rose Coolon and Nathan Vanderveen for mouse colony management.

REFERENCES

1. Rossi DJ, Jamieson CH, Weissman IL. Stems cells and the pathways to aging and cancer. Cell. 2008; 132:681–696. [PubMed: 18295583]
2. Ward AF, Braun BS, Shannon KM. Targeting oncogenic Ras signaling in hematologic malignancies. Blood. 2012; 120:3397–3406. [PubMed: 22898602]
3. Essers MA, et al. IFNalpha activates dormant haematopoietic stem cells in vivo. Nature. 2009; 458:904–908. [PubMed: 19212321]
4. Foudi A, et al. Analysis of histone 2B-GFP retention reveals slowly cycling hematopoietic stem cells. Nat Biotechnol. 2009; 27:84–90. [PubMed: 19060879]
5. Wilson A, et al. Hematopoietic stem cells reversibly switch from dormancy to self-renewal during homeostasis and repair. Cell. 2008; 135:1118–1129. [PubMed: 19062086]

6. Rossi L, et al. Less is more: unveiling the functional core of hematopoietic stem cells through knockout mice. Cell stem cell. 2012; 11:302–317. [PubMed: 22958929]
7. Kamminga LM, et al. The Polycomb group gene Ezh2 prevents hematopoietic stem cell exhaustion. Blood. 2006; 107:2170–2179. [PubMed: 16293602]
8. Liu F, et al. Csf3r mutations in mice confer a strong clonal HSC advantage via activation of Stat5. J Clin Invest. 2008; 118:946–955. [PubMed: 18292815]
9. Yuan Y, Shen H, Franklin DS, Scadden DT, Cheng T. In vivo self-renewing divisions of haematopoietic stem cells are increased in the absence of the early G1-phase inhibitor, p18INK4C. Nat Cell Biol. 2004; 6:436–442. [PubMed: 15122268]
10. Moran-Crusio K, et al. Tet2 loss leads to increased hematopoietic stem cell self-renewal and myeloid transformation. Cancer cell. 2011; 20:11–24. [PubMed: 21723200]
11. Challen GA, et al. Dnmt3a is essential for hematopoietic stem cell differentiation. Nat Genet. 2012; 44:23–31. [PubMed: 22138693]
12. Takizawa H, et al. Enhanced engraftment of hematopoietic stem/progenitor cells by the transient inhibition of an adaptor protein, Lnk. Blood. 2006; 107:2968–2975. [PubMed: 16332975]
13. Buza-Vidas N, et al. Cytokines regulate postnatal hematopoietic stem cell expansion: opposing roles of thrombopoietin and LNK. Genes Dev. 2006; 20:2018–2023. [PubMed: 16882979]
14. Braun BS, et al. Somatic activation of oncogenic Kras in hematopoietic cells initiates a rapidly fatal myeloproliferative disorder. Proceedings of the National Academy of Sciences of the United States of America. 2004; 101:597–602. [PubMed: 14699048]
15. Sabnis AJ, et al. Oncogenic Kras initiates leukemia in hematopoietic stem cells. PLoS Biol. 2009; 7:e59. [PubMed: 19296721]
16. Li Q, et al. Hematopoiesis and leukemogenesis in mice expressing oncogenic NrasG12D from the endogenous locus. Blood. 2011; 117:2022–2032. [PubMed: 21163920]
17. Wang J, et al. Endogenous oncogenic Nras mutation promotes aberrant GM-CSF signaling in granulocytic/monocytic precursors in a murine model of chronic myelomonocytic leukemia. Blood. 2010; 116:5991–6002. [PubMed: 20921338]
18. Zhang Y, Taylor BR, Shannon K, Clapp DW. Quantitative effects of Nf1 inactivation on in vivo hematopoiesis. J Clin Invest. 2001; 108:709–715. [PubMed: 11544276]
19. Wang J, et al. NrasG12D/+ promotes leukemogenesis by aberrantly regulating hematopoietic stem cell functions. Blood. 2013; 121:5203–5207. [PubMed: 23687087]
20. Haigis KM, et al. Differential effects of oncogenic K-Ras and N-Ras on proliferation, differentiation and tumor progression in the colon. Nat Genet. 2008; 40:600–608. [PubMed: 18372904]
21. Kiel MJ, Yilmaz OH, Iwashita T, Terhorst C, Morrison SJ. SLAM Family Receptors Distinguish Hematopoietic Stem and Progenitor Cells and Reveal Endothelial Niches for Stem Cells. Cell. 2005; 121:1109–1121. [PubMed: 15989959]
22. Oguro H, Ding L, Morrison SJ. SLAM Family Markers Resolve Functionally Distinct Subpopulations of Hematopoietic Stem Cells and Multipotent Progenitors. Cell stem cell. 2013; 13:102–116. [PubMed: 23827712]
23. Krebs DL, Hilton DJ. SOCS proteins: negative regulators of cytokine signaling. Stem Cells. 2001; 19:378–387. [PubMed: 11553846]
24. Li LX, Goetz CA, Katerndahl CD, Sakaguchi N, Farrar MA. A Flt3- and Ras-dependent pathway primes B cell development by inducing a state of IL-7 responsiveness. J Immunol. 2010; 184:1728–1736. [PubMed: 20065110]
25. Cui Y, et al. Inactivation of Stat5 in mouse mammary epithelium during pregnancy reveals distinct functions in cell proliferation, survival, and differentiation. Mol Cell Biol. 2004; 24:8037–8047. [PubMed: 15340066]
26. Itzykson R, et al. Clonal architecture of chronic myelomonocytic leukemias. Blood. 2013; 121:2186–2198. [PubMed: 23319568]
27. Kotecha N, et al. Single-cell profiling identifies aberrant STAT5 activation in myeloid malignancies with specific clinical and biologic correlates. Cancer Cell. 2008; 14:335–343. [PubMed: 18835035]

28. Matsuda K, et al. Spontaneous improvement of hematologic abnormalities in patients having juvenile myelomonocytic leukemia with specific RAS mutations. Blood. 2007; 109:5477–5480. [PubMed: 17332249]

29. De Filippi P, et al. Germ-line mutation of the NRAS gene may be responsible for the development of juvenile myelomonocytic leukaemia. Br J Haematol. 2009; 147:706–709. [PubMed: 19775298]

30. Kraoua L, et al. Constitutional NRAS mutations are rare among patients with Noonan syndrome or juvenile myelomonocytic leukemia. Am J Med Genet A. 2012; 158A:2407–2411. [PubMed: 22887781]

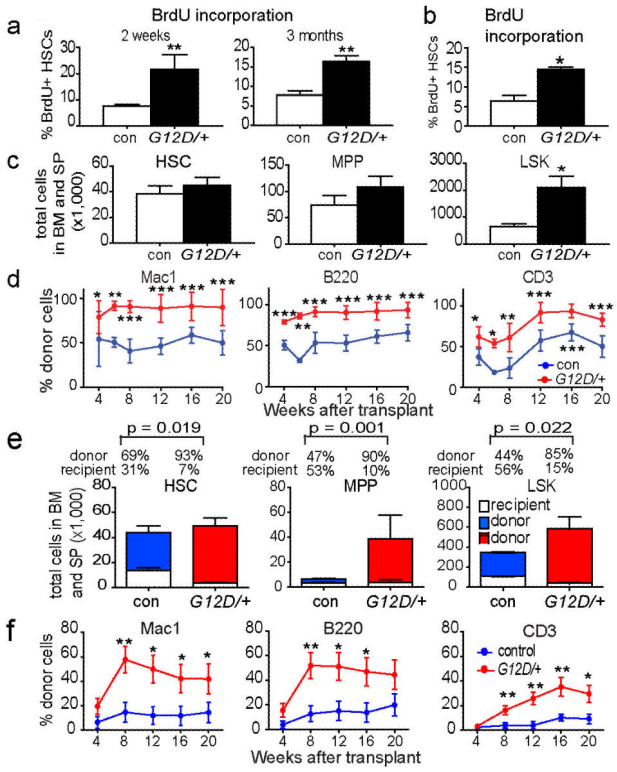

Figure 1. ***Nras*$^{G12D/+}$ increased HSC proliferation and competitiveness**

a) A 24-hour pulse of BrdU was administered to *Mx1-cre; Nras*$^{G12D/+}$ (G12D/+) and littermate control (con) mice at 2 weeks and 3 months after pIpC treatment (n=3 mice/treatment). **b**) BrdU incorporation by CD150^{+}CD48^{-}LSK HSCs from *Vav1-Cre; Nras*$^{G12D/+}$ mice (G12D/+) or littermate controls (con) at 6-10 weeks of age (n=3). **c**) The total number of CD150^{+}CD48^{-}LSK HSCs, CD150^{-}CD48^{-}LSK MPPs, and LSK cells in the bone marrow and spleens of *Mx1-cre; Nras*$^{G12D/+}$ (G12D/+) and littermate control (con) mice at 2 weeks after pIpC treatment (n=5 mice/treatment). **d**) 5×10^{5} donor bone marrow cells from *Mx1-cre; Nras*$^{G12D/+}$ (G12D/+) or littermate control (con) mice at 2 weeks after pIpC treatment (n=3 donors/genotype) were transplanted into irradiated recipient mice (n=15 recipients/genotype) along with 5×10^{5} recipient bone marrow cells. Donor cell reconstitution in the myeloid (Mac-1^{+} cells), B (B220^{+}), and T (CD3^{+}) cell lineages for 4 to 20 weeks after transplantation. **e**) Recipients of *Mx1-cre; Nras*$^{G12D/+}$ (G12D/+) bone marrow cells (n=5) had significantly ($p<0.05$) higher proportions of donor-derived HSCs, MPPs and LSK cells compared to recipients of control bone marrow cells (con). **f**) 10 donor HSCs from *Mx1-cre; Nras*$^{G12D/+}$ (G12D/+) or littermate control (con) mice at 2 weeks after pIpC treatment (n=3 donors/genotype) were transplanted into irradiated recipient mice (n=14 recipients/genotype) along with 3×10^{5} recipient bone marrow cells. Data represent mean±s.d.. Two-tailed student's t-tests were used to assess statistical significance. *P<0.05, **P<0.01, ***P<0.001.

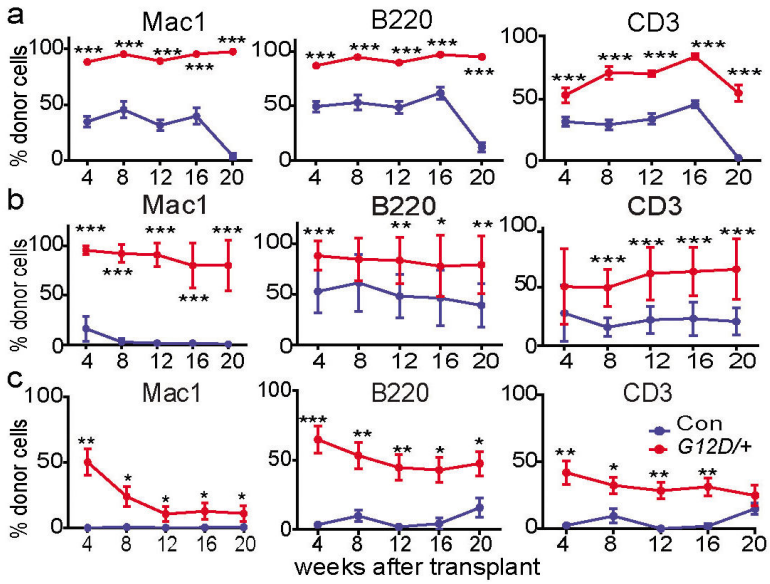

Figure 2. *Nras*$^{G12D/+}$ increased HSC and MPP self-renewal

a) Secondary transplantation (n=19 recipients/genotype) of 3×10^6 bone marrow cells from primary recipient mice in Figure 1c (n=4 donors/genotype). Donor cell reconstitution in the myeloid (Mac-1$^+$), B (B220$^+$), and T (CD3$^+$) cell lineages for 4 to 20 weeks after transplantation **b**) Transplantation of 3×10^6 bone marrow cells from secondary recipient mice in Figure 2a (n=3 donors/genotype) into tertiary recipient mice (n=8 recipients for control and 9 recipients for *Nras*$^{G12D/+}$) **c**) Transplantation of 3×10^6 bone marrow cells from tertiary recipient mice (n=3 donors for control and 4 donors for *Nras*$^{G12D/+}$) in **Figure 2b** into quaternary recipient mice (n=7 recipients for control and 17 for *Nras*$^{G12D/+}$). Each serial transplant was performed at 20 weeks after the prior round of transplantation. Data represent mean±s.d.. Two-tailed student's t-tests were used to assess statistical significance. *P<0.05, **P<0.01, ***P<0.001.

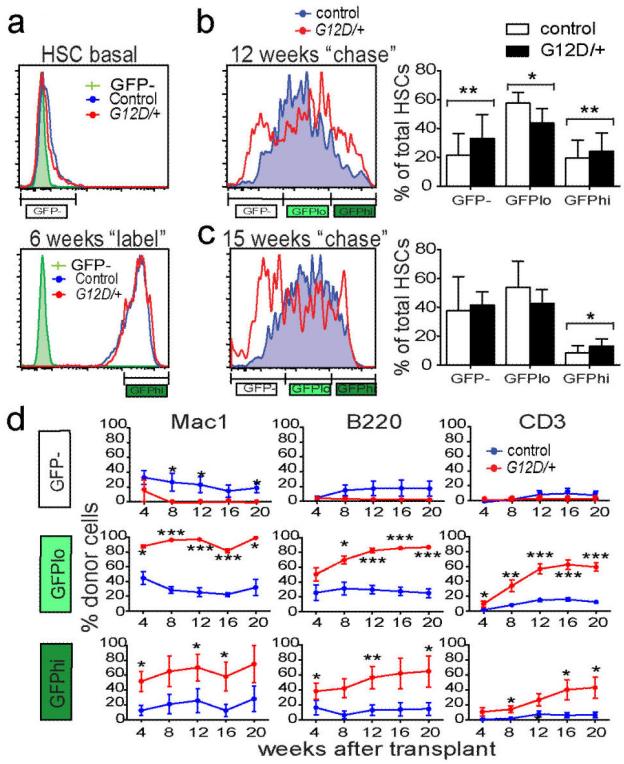

Figure 3. ***Nras*$^{G12D/+}$ has a bimodal effect on HSC cycling**

a) GFP expression in HSCs from *Mx1-cre; Nras*$^{G12D/+}$; *Col1A1-H2B-GFP; Rosa26-M2-rtTA* mice (G12D/+) and littermate controls (control) without doxycycline treatment (n=3, left), or after 6 weeks of doxycycline treatment (n=3, right). **b**) GFP expression in HSCs from age and sex-matched pairs of *Nras*$^{G12D/+}$ and control mice after labeling followed by 12 weeks of chase without doxycycline (n=8 pairs of mice from 8 independent experiments; $p<0.05$ by two-way ANOVA and posthoc pairwise t-tests). Despite overlapping standard deviations, differences were statistically significant in pairwise t-tests because the frequencies of H2B-GFP^{-} HSCs and H2B-GFP^{hi} HSCs were always higher in the *Nras*$^{G12D/+}$ mice. **c**) GFP expression in HSCs from pairs of age and sex-matched *Nras*$^{G12D/+}$ and control mice after 15 weeks of chase without doxycycline (n=7 mice from 5 independent experiments). *Nras*$^{G12D/+}$ mice always had higher frequencies of H2B-GFP^{hi} HSCs ($p<0.05$ by pairwise t-tests). **d**) We transplanted 15 CD150^{+}CD48^{-}LSK H2B-GFP^{hi} HSCs, 50 H2B-GFP^{lo} HSCs, or 75 H2B-GFP^{-} HSCs from *Nras*$^{G12D/+}$ or littermate control mice after 12 weeks of chase into irradiated wild-type recipients along with 3×10^{5} recipient bone marrow cells (2 independent experiments with a total of 7 recipients/genotype). Data represent mean±s.d.. Unless otherwise stated, two-tailed student's t-tests were used to assess statistical significance. *P<0.05, **P<0.01, ***P<0.001.

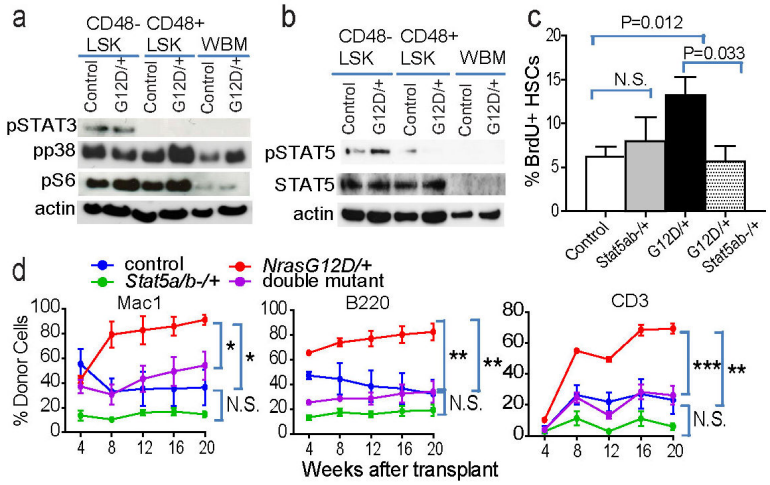

Figure 4. Increased STAT5 activation mediates the effect of Nras$^{G12D/+}$ on HSCs

Western blots for pSTAT3, pp38, pS6, and ß-actin (**a**) and pSTAT5, total STAT5 and ß-actin (**b**) (two additional experiments are shown in Supplementary figure 8j). Cells were stimulated in culture with SCF and TPO for 30 minutes before protein extraction. **c**) The frequency of BrdU^{+}CD150^{+}CD48^{-}LSK HSCs after a 24-hour pulse of BrdU to *Mx1-cre; Stat5ab$^{fl/+}$* (*Stat5ab$^{-/+}$*) mice, *Mx1-cre; Nras$^{G12D/+}$* (G12D/+) mice, *Mx1-cre; Nras$^{G12D/+}$; Stat5ab$^{fl/+}$* (*G12D/+; Stat5ab$^{-/+}$*) compound mutant mice, or control mice (n=4). **d**) 5×10^{5} donor bone marrow cells from mice of each genotype were transplanted into irradiated recipients along with 5×10^{5} recipient bone marrow cells (2 independent experiments with a total of 8 recipients/genotype). Data represent mean±s.d.. Two-tailed student's t-tests were used to assess statistical significance.